Methods for High Power EM Pulse Measurement

Petr DREXLER, Pavel FIALA

Dept. of Theoretical and Experimental Electrical Engineering, Brno University of Technology,
Kolejní 2906/4, 612 00 Brno, Czech Republic

fialap@feec.vutbr.cz, xdrexl00@stud.feec.vutbr.cz

Abstract. *There are some suitable methods for the measurement of ultra-short solitary electromagnetic pulses that can be generated by high power pulsed generators. The measurement methods properties have to correspond to the fact whether we want to measure pulses of voltage, current or free-space electromagnetic wave. The need for specific measurement methods occurred by the development of high power microwave pulse generator* [1]. *Applicable methods are presented in this paper. The method utilizing Faraday's induction law allows the measurement of generated current. For the same purpose the magneto-optic method can be utilized, with its advantages. For measurement of output microwave pulse of the generator the calorimetric method was designed and realized.*

Keywords

Electromagnetic pulse, high power microwave generator, calorimetric method, magneto-optical effect, vircator.

1. Introduction

Fig. 1. shows the basic principle of microwave pulsed power generator. It consists of three stages – the primary source of electrical energy, the pulsed power generator and the microwave pulsed power generator (load in Fig. 1). The primary source supplies the pulsed power generator which ensures the pulse current amplification. After transformation to the high voltage and pulse shaping (not shown in Fig. 1), the pulse is fed to the microwave pulsed power generator. The detailed description of pulsed power generation can be found in [2].

For example, the peak level of current pulse achieves the value of I_p = 100 kA with the pulse duration t_d = 70 μs typically in the second stage. After high voltage transformation and using pulse shaping element we can get a voltage pulse with the peak value U_p = 400 kV and with the rise time t_r = 0.1 ns. Following microwave source (vircator [3]*)* emits electromagnetic pulse (EMP). The characteristic of EMP is high power level (P_{max} = 250 MW [1]) and very short time duration ($t_p \in$ <1, 60> ns).

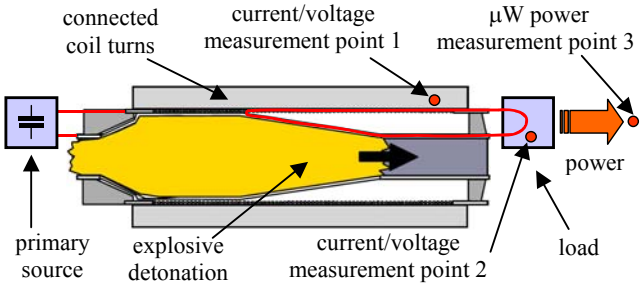

Fig. 1. The basic principle of microwave pulsed power generator.

For the pulsed power generator evaluation it is essential to obtain an idea about the qualitative and quantitative processes during the generator operation. Important measurement points are shown in Fig. 1. Special requirements for measurement methods have to be considered because of the specific pulses properties.

2. Methods for Pulses Identification

The basic quantity of interest is the current of the pulsed power generator. It is quite difficult to use the classical methods for current measurement (shunt) because of the high current level. The measurement of the induced magnetic field has been proposed, according to the Faraday's induction law.

The most straightforward way for the voltage pulse measurement is the method using high voltage divider. An inductance-free high voltage divider has been developed. This divider is suitable for single shot application [4].

The final product of the relativistic vircator effect [3] is the electromagnetic pulse, which can be guided in a cylindrical waveguide or emitted into the free-space. However, it was not possible to use a microwave probe or antenna for the first vircator test. The frequency range and the mode distribution were unknown. The calorimetric measurement method was proposed for the vircator tests. We can't get the pulse waveform using the calorimetric method. On the other side, it allows physically correct power and energy measurement. The power of the EMP is the crucial parameter, which gives an idea about vircator optimal design.

2.1 Method Based on Faraday's Induction Law

Current measurement method is based on the application of the Faraday's induction law where the pulse is located by a sensor (the coil with $N_s = 1 \div 50$ turns). The signal induced in the coil is led to the recording device, generally an oscilloscope. Due to safety requirements, the distance between the sensor and the oscilloscope is $l = 50$ m. This parameter introduces quality decrease of the recorded information in the way of the signal amplitude reduction, change of the signal phase and the pulse prolongation.

The elimination of this limitation is in Method I, depicted in Fig. 2, made by backward correction exploiting the Laplace transform. Pulses up to limit pulse length $T_{max} = 1$ ns were measured by this method and magnetic flux ϕ was evaluated [1].

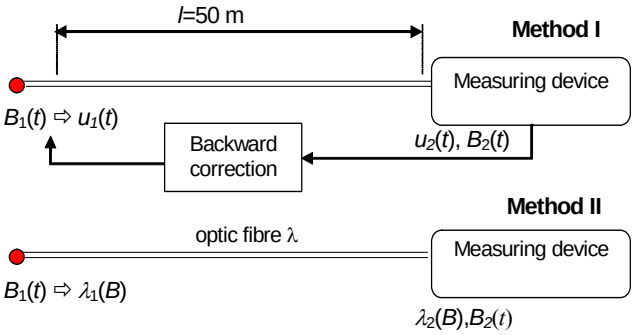

Fig. 2. Principles of the methods based on Faraday's induction law and magnetooptic effect.

Fig. 3. shows the installation of the sensor coils on the generator prototype by its test. Coils are of Rogowski type and they are connected via coaxial cable to the recording device. The example of the current pulse waveform obtained by the first experiments with the coil sensor is shown in Fig. 4.

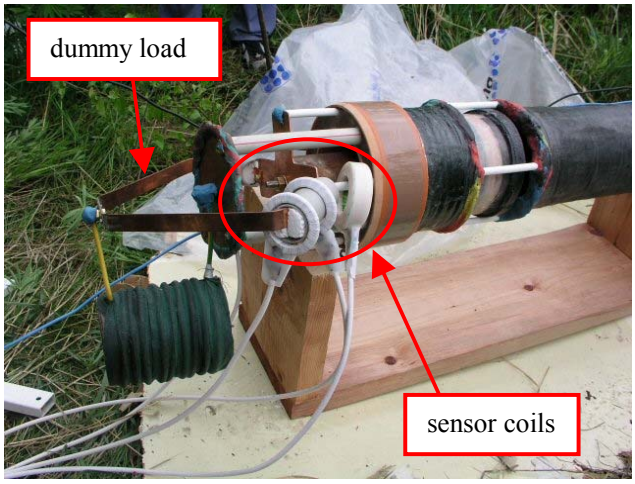

Fig. 3. Installation of the sensor coils by the pulsed power generator test.

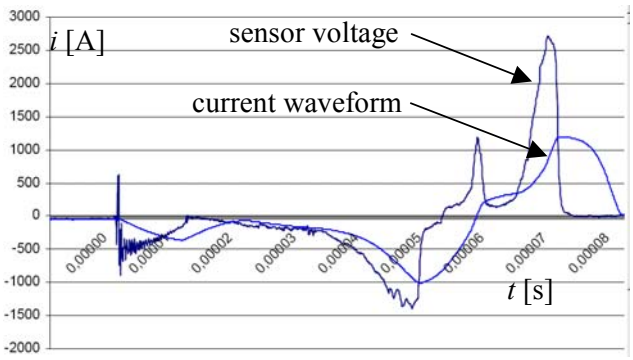

Fig. 4. An example of the current pulse waveform.

2.2 Method Based on Magneto/Electro-Optic Effect

The second method presented – the magnetooptic method – uses the Faraday's magnetooptic (Kerr's electrooptic) effect as a sensor principle. The sensor utilizing the magnetooptic method is in development. The connection between the sensor and the measuring device is implemented in the optical wavelength as shown in Fig. 2.

There are three basic types of the possible active sensors. The first type is a garnet with high Verdet constant, the second one is an optic fiber and the third one is based on magnetooptic properties of ferromagnetic mono/multi thin film. Other types of Version IV sensors are based on the magnetooptic Kerr's effects (MOKE), or surface MOKE (SMOKE) effect. By an available measuring devices application we can measure pulses with the limit length up to $T_{max} = 0.01$ ns [5] for repetitive pulse train.

2.3 Calorimetric Methods

The above mentioned methods indicate the electromagnetic parts of the wave – electric or magnetic. They don't express the power conditions of the electromagnetic wave. For some of the measurement it is essential to evaluate power flow through the defined area.

The group of calorimetric methods represents another type of converter to be introduced. We can measure power supplied by a pulse (Poynting´s vector) when we use the calorimetric converter. The sensor is connected to the measuring device (oscilloscope) by a coaxial cable of $l = 50$ m length. Fig. 5. depicts four versions of the method utilizing calorimetric measurement.

Version I discussed in [6,7] has a sensor in the form of an ideal resistor and enables measurement of the maximum value of microwave power P_{max}. The analyzed peak voltage corresponds to peak value of power P_{max}. For available measuring devices we can measure pulses with the limit length $T_{max} = 50$ ps.

Version II scans the change of resistance of the sensor, created by an evaporated thin layer, in dependence

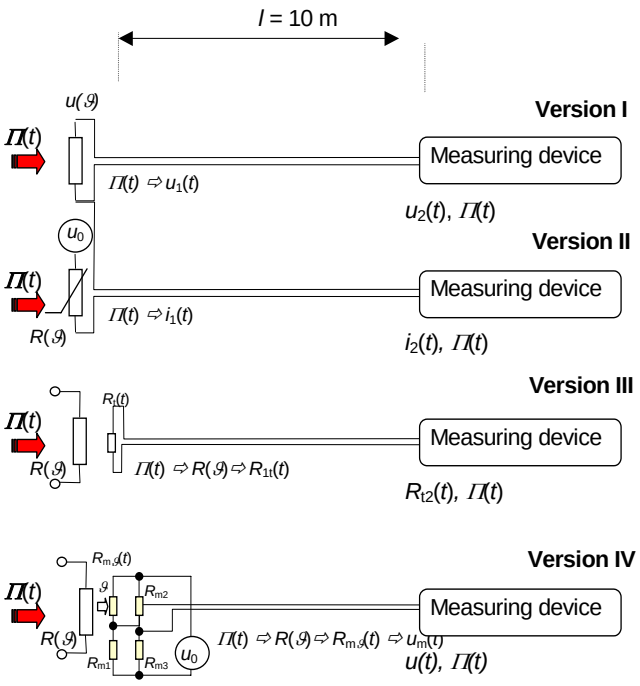

Fig. 5. Calorimetric measurement of the solitary pulse power.

on the pulse energy. For available measuring devices we can reach the accuracy of 30 % up to impulse limit length T_{max} = 0.1 ns.

Version III is based on the measurement of the temperature change of the thermistor placed in contact with the layer. Under the same conditions as for the previous version we can reach the accuracy improvement of an order of magnitude.

Version IV is the bridge connection of version III. Several thermistors are attached in series to the evaporated layer; then, three resistors create a DC bridge of Weston type with the thermistors. The change of resistance in the thermistor arm is evaluated. The voltage in the measuring bridge diagonal is consequently integrated. Thus, the value of the pulse energy is obtained (and recorded by the measuring device). For available measuring devices we can measure pulses with the limit length T_{max} = 0.03 ns with accuracy to 10 %.

3. Used Calorimetric Method

The calorimetric sensor was of the disc design. The carbon with changed crystal lattice was designed for use as one of the thin layer types.

3.1 Mathematical Model

It is possible to carry out an analysis of the calorimetric sensor model as a numerical solution by means of the Finite element method (FEM). The electromagnetic part of the model is based on the solution of full Maxwell's equations

$$\nabla\times\boldsymbol{E}=-\frac{\partial\boldsymbol{B}}{\partial t},\nabla\times\boldsymbol{H}=\sigma\boldsymbol{E}+\frac{\partial\boldsymbol{D}}{\partial t}+\boldsymbol{J},\nabla\cdot\boldsymbol{D}=\rho,\nabla\cdot\boldsymbol{B}=0 \text{ in } \Omega, \quad (1)$$

where $\boldsymbol{E}$ and $\boldsymbol{H}$ are the electrical field intensity vector and the magnetic field intensity vector, $\boldsymbol{D}$ a $\boldsymbol{B}$ are the electrical field density vector and the magnetic flux density vector,, $\boldsymbol{J}_s$ is the current density vector of the sources, ρ is the density of free electrical charge, γ is the conductivity of the material and Ω is the definition area of the model. The relationships between electrical and magnetic field intensities and densities are given by material relationships

$$\boldsymbol{D}=\varepsilon\boldsymbol{E}, \qquad \boldsymbol{B}=\mu\boldsymbol{H}. \quad (2)$$

The permittivity ε, the permeability μ and the conductivity γ in HFM are generally tensors with main axes in the direction of the Cartesian coordinates x, y, z. When all the field vectors perform rotation with the same angular frequency ω, it is possible to rewrite the first Maxwell equations

$$\nabla\times\underline{\boldsymbol{E}}=-j\omega\mu\underline{\boldsymbol{H}},\ \nabla\times\underline{\boldsymbol{H}}=(\sigma+j\omega\varepsilon)\underline{\boldsymbol{E}}+\underline{\boldsymbol{J}}_s \text{ in } \Omega, \quad (3)$$

where $\underline{\boldsymbol{E}}$, $\underline{\boldsymbol{H}}$, $\underline{\boldsymbol{J}}_s$ are field complex vectors. Taking into account boundary conditions given in (1) and after rearranging (3) we get

$$(j\omega)^2\varepsilon\underline{\boldsymbol{E}}+\sigma\underline{\boldsymbol{E}}+\nabla\times\mu^{-1}\nabla\times\underline{\boldsymbol{E}}=-j\omega\underline{\boldsymbol{J}}_s. \quad (4)$$

We apply Galerkin's method with vector approximation functions $\boldsymbol{W}_i$ and use vector form of the Green theorem on the double rotation element [3]. After discretization we get the expression

$$-k_0[M]\{\boldsymbol{E}\}+jk_0[C]\{\boldsymbol{E}\}+[K]\{\boldsymbol{E}\}=\{\boldsymbol{F}\}, \quad (5)$$

where $\{\boldsymbol{E}\}$ is the column matrix of electrical intensity complex vectors. The matrixes $[K]$, $[C]$ and $[M]$ are in the form that is given in manual [4] and vector $\{\boldsymbol{F}\}$ is evaluated from the expression

$$\{\boldsymbol{F}\}=-jk_0Z_0\int_{\Omega}[\boldsymbol{W}_i]\{\boldsymbol{J}_s\}d\Omega+jk_0Z_0\int_{\Gamma_0+\Gamma_1}[\boldsymbol{W}_i]\{\boldsymbol{n}\times\boldsymbol{H}\}d\Gamma. \quad (6)$$

Vector approximation functions $\boldsymbol{W}$ are given in manual [4]; k_0 is the wave number for vacuum, Z_0 is the impedance of free space. The set of equations (5) is independent of time and gives $\underline{\boldsymbol{E}}$. For transient vector $\boldsymbol{E}$ we can write

$$\boldsymbol{E}=\mathrm{Re}\left\{\underline{\boldsymbol{E}}\,\mathrm{e}^{\mathrm{j}\omega t}\right\}. \quad (7)$$

3.2 Model in ANSYS

The geometrical model was created with standard tools in ANSYS using the automated generator of mesh and nodes; then the mathematical model is formed. The applied element is HF120.

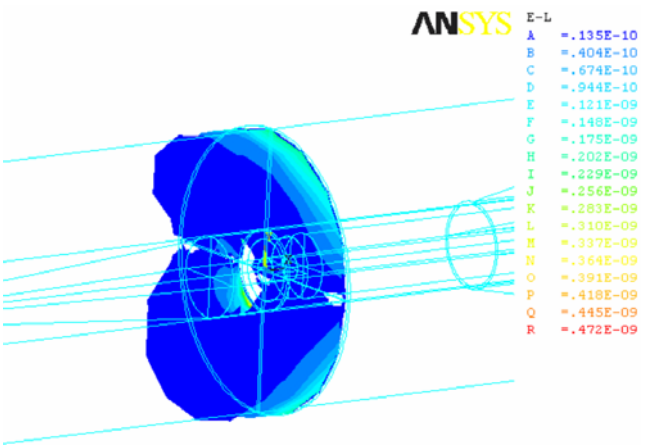

Fig. 6. Evaluation of the module of magnetic intensity *H*.

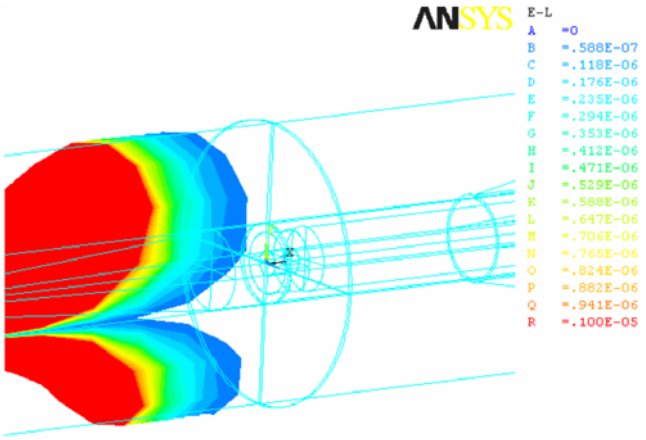

Fig. 7. Evaluation of the module of electric intensity *E*.

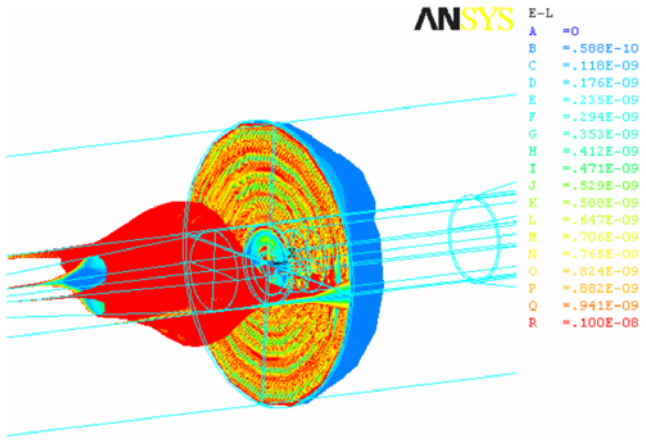

Fig. 8. Evaluation of the module of electric intensity *E*.

3.3 Results of the Analysis

In Fig. 6. and Fig. 7. the modules of vector functions magnetic field density *B* and intensity *E* are shown. There are interesting results of the HF converter wave from TE, TM type of wave to TEM wave. The results are shown for the first harmonic part of the pulse with f_1=3.9GHz, input electric field with intensity E_x=100V/m. We can show the quality of electromagnetic absorber with one result in Fig. 8. There, a good result of absorption is visible.

4. Realization of the Calorimetric Sensor

Pursuant to the results obtained by numerical analysis, the calorimetric sensor was built. The prototype of the sensor was designed for the measurement of vircator with output power of P_{max} = 250 MW, length of pulse $t_p \in$<10, 60> ns. A vircator is a pulse high-energy source of microwave energy based on the virtual cathode effect; its experimental construction is shown in Fig. 9. Fig.10. shows the waveform of vircator's anode current by initiation.

Fig. 9. Experimental construction of a vircator, P_{max} = 250 MW.

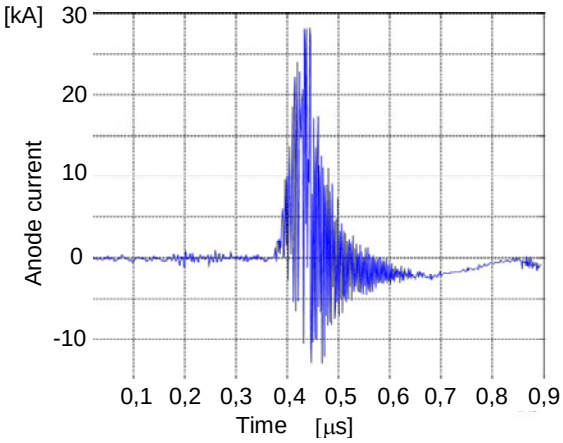

Fig. 10. Waveform of vircator's anode current.

The concept was designed after consultation [8] for the supposed power and pulse length with a room for absorption and damping of the possible back EMG wave.

4.1 Waveguide-Fitted Calorimetric Sensor

The first prototype of the calorimetric sensor was intended for waveguide connection with a microwave vircator. Fig. 11 depicts the principle scheme of the calorimetric sensor design. Fig.12 shows the outer shell. The purpose of the sensor was to measure the energy (power) of the emitted EMP. It was not possible to use the probe because the modes of the field, waveform and spectrum were not known.

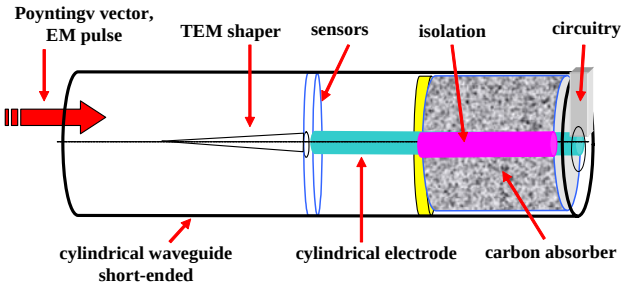

Fig. 11. Principal scheme of the calorimetric sensor.

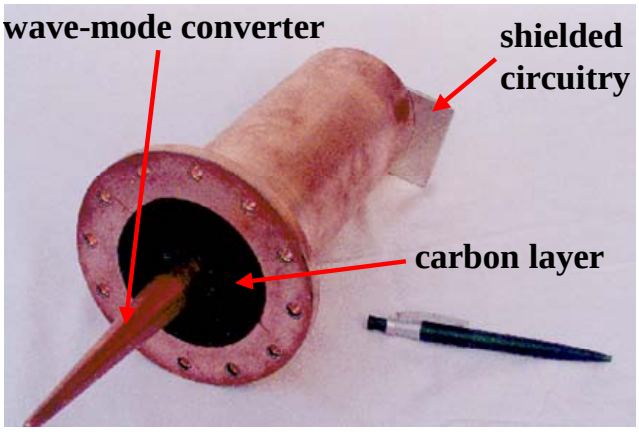

Fig. 12. Waveguide-fitted calorimetric sensor.

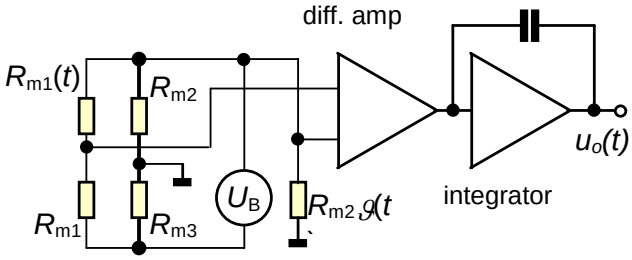

Fig. 13. Principle scheme of the sensor circuitry.

The sensor circuitry (Fig. 13) works as an integrator. The diagonal voltage on the thermistor bridge is proportional to the carbon layer temperature. The voltage from the bridge is fed to the differential amplifier which helps to suppress the influence of thermal fluctuations with the help of vicinity temperature sensor. The output signal is integrated by an amplifier with an automatic offset compensation. The integral of the calorimeter voltage is proportional to the absorbed pulse energy, as shown in Fig.14.

4.2 Free-Space Combined Calorimetric Sensor

For the measurement of free-space vircator EMP, the new combined calorimetric sensor was built. The sensor operation is based on the version I and version IV of the calorimetric method in Fig. 5. The first part (version I) serves as the sensor of instantaneous power and the second part (version IV) serves as the sensor of pulse energy.

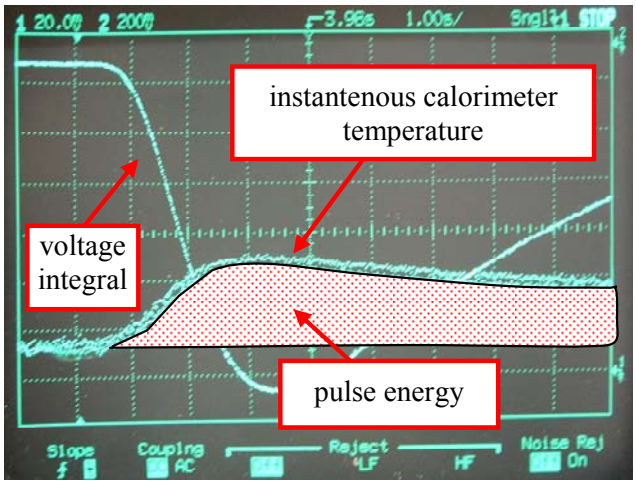

Fig. 14. The output voltage of the calorimeter and its integral.

The realization of the combined sensor is shown in Fig. 15. Both parts are equipped with Horn antennas to ensure the matching of the free-space EMG wave to the sensor input. The parameters of the antenna obtained by the help of numerical simulation are following [9]:

Gain: $G = 19$ dB
3dB beam angle: $\theta_{3dB} = 21°$
6dB beam angle: $\theta_{6dB} = 30°$
Front-to-back ratio: FBR = 69.4

The radiation pattern of the Horn-type antenna in dB is shown in Fig. 16

Fig. 15. Realization of optimized combined calorimetric sensor.

The sensor was calibrated with an RF generator in a semi-anechoic room in VTUPV Vyškov, Fig. 17. The calibration was performed for microwave pulses with defined duration and power level, with the frequencies f=3, 4, 5, and 6 GHz. The power level and pulse duration relation were set for the emitted energy $F_{test} \in$ <0,1; 10> J.

Due to safety requirements, the connection between the sensor and the measuring device was ensured by means of a coaxial cable of the minimum length $l_{min} = 10$ m.

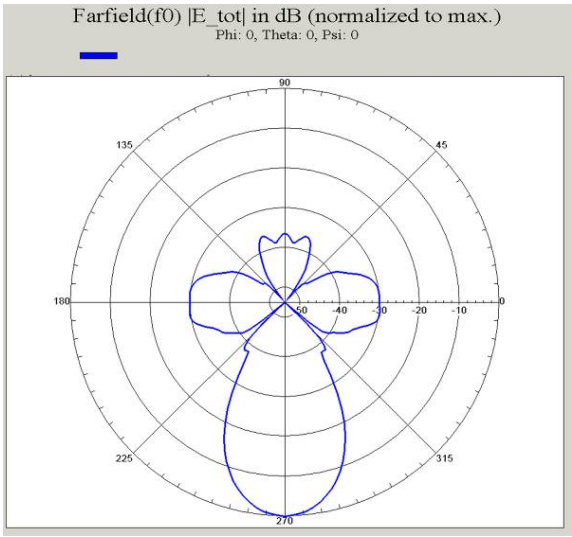

Fig. 16. Radiation pattern of Horn-type antenna in dB.

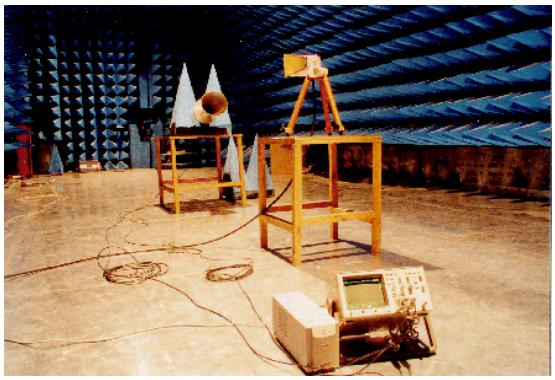

Fig. 17. Calibration of the calorimetric sensor.

The combined calorimetric sensor was used for the measurement of vircator-emitted EMP. The supply of the vircator was provided by a pulse high-voltage source powered by Marx bank. When the vircator is in the operational mode, hard RTG emission is generated in addition to the microwave emission. The energy of the electron beam is $W_b = 1$ MeV. Therefore, safety requirements equal to those mentioned above have to be considered.

The waveform of the measured small microwave power is in Fig. 18. The peak value of the vircator-emitted EMP reached $P_{max} = 50$ kW in this experiment. However, the vircator is able to emit EMP with a peak value of hundreds of MW when supplied with pulsed power generators.

5. Design of the Magnetooptic Method

The magnetooptic (MO) method is proposed for further experiments. The magnetooptic method allows ultra-short pulses waveform measurement because of its high bandwidth. The polarization rotation of light passing the MO sensor is affected by the magnetic part of EM pulse. The rotation is due to the magnetic field and properties of the sensor material (Verdet constant). For the measurement the MO garnet, glass or thin film may be used [10].

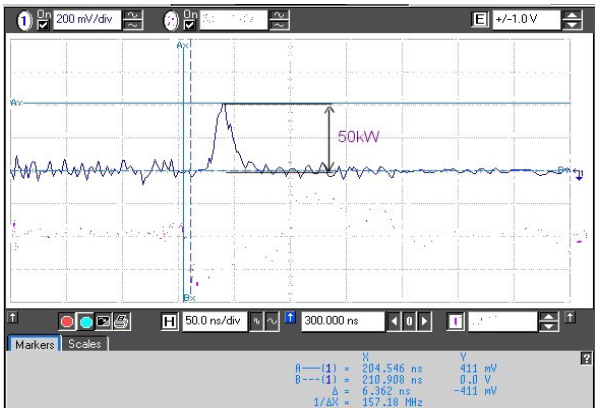

Fig. 18. Measured waveform of small microwave power, $P_{max} = 50$ kW.

The absolute measurement method utilizing the MO glass element was experimentally realized with low frequency magnetic field. Laser beam with linear polarization passes the MO glass placed in Helmholtz coil. The laser beam is subsequently fed through an analyzer and the polarization rotation is converted to intensity modulation. The intensity of light is sensed by a photodiode. The magnetooptic glass FR-5 by Hoyoa Optics was used in this experiment. Fig. 19 shows the MO element in the holder.

Next, the differential method was experimentally realized [11]. The differential method utilizes Wollaston prism and offers better sensitivity. It is proposed for the next pulse current sensor development. The experiment for the measurement of high frequency magnetic field is in development – Fig. 20.

The sensitivity of the sensor and its bandwidth are contradictory properties. Because of the high power level of EM pulse the sensitivity of the sensor is not a critical requirement. The bandwidth of the sensor has to be appropriate to the measured signal characteristic – it has to be able to detect transients with duration 1 ns. The corresponding bandwidth for this requirement reaches the value of 350 MHz.

6. Conclusion

The overview of several methods suitable for the measurement of short solitary pulses with high power level was given. The characteristics of the designed method were discussed. Some methods were experimentally tested and evaluated. A combined calorimetric sensor for free-space measurement was built and the functionality of the calorimetric sensor was proved by real measurement of vircator-emitted EMP.

Fig. 19. Magnetooptic element (FR-5) in the holder.

Fig. 20. Experimental setup for high frequency magnetic field measurement.

Acknowledgements

The paper was prepared within the framework of the research plan No. MSM 0021630513 of the Ministry of Education, Youth and Sports of the Czech Republic.

References

[1] FIALA, P. *Non-conventional sources of electrical energy.* Brno: BUT FEKT, 2003.

[2] FIALA, P., DREXLER, P., RYCHNOVSKÝ, J. *Pulsed Power Generator with Output Power up to 20GW*. Research report. HS Prototypa a.s., 18580001.

[3] BARKER, R. J., SCHAMILOGLU, E. *High-Power Microwave Sources and Technologies*. IEEE Press, 2001.

[4] DREXLER, P., KALÁB, P., FIALA, P. Inductance-free high voltage divider for extreme conditions. In *Proceeding of 16th International Conference on Dielectric and Insulating Systems in Electrical Engineering 2006.* Častá-Píla (Slovakia), 2006, p. 168.

[5] RIORDAN, J. A., SUN, F.G., LU, Z.G., ZHANG, X.-C. Free-space transient magneto-optic sampling. *Applied Physics Letters.* 1997, vol. 71, p. 1452-1454.

[6] KASAL, M. *Multinuclear Measuring Channel of NMR Spectrometer.* Brno: FE BUT, 1984.

[7] PFEFFER, M., KASAL, M. Automatic Impulse Reflectometer. *Sdělovací technika,*. 1986, vol. 10/11 (in Czech).

[8] ŠUNKA, P. Verbal information. UFP AV ČR, Praha 6, 2003.

[9] PALÍŠEK, L. *The Alternative to Anti-Infantry Mines*. Research report. VOP26, Šternberk. VTUPV Vyškov, 2005.

[10] CRAIG, A. E., CHANG, K. *Optical Modulation: Magneto-Optical Devices. Handbook of Optical Components and Engineering.* New Jersey: John Wiley & Sons, Inc., 2003. 1380 pages. ISBN 0-471-39055-0

[11] DREXLER, P. *Methods for the Measurement of Ultrashort Electromagnetic Pulses*. Treatise on the Ph.D. thesis. BUT FEKT, Brno, 2006.

About Authors...

Petr DREXLER graduated from the Faculty of Electrical Engineering and Communication, Brno University of Technology, electronics engineering. Since 2004 he has been with the Department of Theoretical and Experimental Electrical Engineering, Brno University of Technology. At present he is pursuing his doctoral degree. His area of interest lies in researching the electro/magnetooptical methods in the measurement of fast pulse electromagnetic fields, the design of optoelectronic circuits and properties of electro/magnetooptical sensors. He is a member of the ICS.

Pavel FIALA received Ph.D. in electrical engineering from the Brno University of Technology, Faculty of Electrical Engineering and Communication in 1998. He joined the Department of Theoretical and Experimental Electrical Engineering in 1990 as a research assistant. Since 2003 he has been an Associate professor and head of the Department of Theoretical and Experimental Electrical Engineering. Dr. Fiala is interested in modeling and analysis of coupled problems by numerical method formulated with partial differential equations using the finite element method (FEM), the boundary element method, the finite difference method. In modeling and optimization, he introduced coupled electromagnetic-thermal-mechanical deformation of lumped parameters models. Also, Pavel Fiala has participated in a large number of industrial projects (ABB EJF, PROTOTYPA, ELEN Brno, FISCHER). He has solved projects of the Ministry of Industry and Business – Pulsed power sources, Alternative to anti-infantry mines, Technology of non-lethal weapons. He is a co-director of the European project WISE – wireless sensing, of the 6th framework dealing with sensor research and sensor development for aeronautics and cosmonautics (participant consortium EADS, DASSAULT, AVIATION, Eurocopter, etc.). He is a member of the IEEE, IEE, OSA, APS, SPIE and a reviewer of the IEEE Sensor Journal.